



Three-dimensional evaluation of the transverse rotator cuff muscle's resultant force angle in relation to scapulohumeral subluxation and glenoid vault morphology in nonpathological shoulders

Xavier Lannes, MD^{a,*}, Patrick Goetti, MD^a, Matthieu Boubat, MSc^b,
Pezhman Eghbali, MSc^b, Fabio Becce, MD^c, Alain Farron, MD^a,
Alexandre Terrier, PhD^{a,b}

^aService of Orthopedics and Traumatology, Lausanne University Hospital and University of Lausanne, Lausanne, Switzerland

^bLaboratory of Biomechanical Orthopedics, Ecole Polytechnique Fédérale de Lausanne, Lausanne, Switzerland

^cDepartment of Diagnostic and Interventional Radiology, Lausanne University Hospital and University of Lausanne, Lausanne, Switzerland

Background: Static posterior subluxation of the humeral head (SPSH) results in glenohumeral osteoarthritis. Treatment strategies for SPSH with or without resulting osteoarthritis remain challenging. There is growing interest in evaluating the rotator cuff muscle volume, fatty infiltration, or forces in osteoarthritic shoulders with SPSH, mainly due to a possible transverse force imbalance. In nonpathological shoulders, the transverse angle of the rotator cuff muscle's resultant force may be associated with scapulohumeral alignment and glenoid vault morphology, despite an assumed transverse force balance. The purpose of this study was to assess the transverse rotator cuff muscle's resultant force angle (TRFA) and its relationship with the scapulohumeral subluxation index (SHSI) and selected glenoid vault parameters using computer modeling.

Methods: Computed tomography scans of 55 trauma patients (age 31 ± 13 years, 36 males) with nonpathological shoulders were analyzed and all measurements performed in 3-dimension. We placed landmarks manually to determine the humeral head center and the rotator cuff tendon footprints. The contours of the rotator cuff muscle cross-sectional areas were automatically predicted in a plane perpendicular to the scapula. Each rotator cuff muscle was divided into virtual vector fibers with homogeneous density. The resultant force vector direction for each muscle, corresponding to the rotator cuff action line, was calculated by vectorially summing the normalized fiber vectors for each muscle, weighted by the muscle trophic ratio. The resultant force vector was projected on the axial plane, and its angle with the mediolateral scapular axis was used to determine TRFA. The SHSI according to Walch, glenoid version angle (GVA), glenoid anteroposterior offset angle (GOA), glenoid depth, glenoid width, and glenoid radius were also evaluated.

This study was approved by the institutional ethics committee (Commission Cantonale d'éthique de la Recherche sur l'être Humain, CER-VD protocol no. 2020-01895), with the waiver of patient informed consent.

*Reprint requests: Xavier Lannes, MD, Service of Orthopedics and Traumatology, Lausanne University Hospital and University of Lausanne, Avenue Pierre Decker 4, Lausanne 1011, Switzerland.

E-mail address: Xavier.Lannes@chuv.ch (X. Lannes).

Results: The mean values for TRFA, SHSI, GVA, GOA, glenoid depth, glenoid width, and glenoid radius were $7.4 \pm 4.5^\circ$, $54.3 \pm 4.8\%$, $-4.1 \pm 4.4^\circ$, $5.1 \pm 10.8^\circ$, 3.3 ± 0.6 mm, 20 ± 2 mm, and 33.6 ± 4.6 mm, respectively. The TRFA correlated strongly with SHSI ($R = 0.731$, $P < .001$) and GVA ($R = 0.716$, $P < .001$) and moderately with GOA ($R = 0.663$, $P < .001$). The SHSI was strongly negatively correlated with GVA ($R = -0.813$, $P < .001$) and moderately with GOA ($R = -0.552$, $P < .001$). The GVA correlated strongly with GOA ($R = 0.768$, $P < .001$). In contrast, TRFA, SHSI, GVA, and GOA did not correlate with glenoid depth, width, or radius.

Conclusion: Despite an assumed balance in the transverse volume of the rotator cuff muscles in nonpathological shoulders, variations exist regarding the transverse resultant force depending on the SHSI, GVA, and GOA. In healthy/nonosteoarthritic shoulders, an increased glenoid retroversion is associated with a decreased anterior glenoid offset.

Level of evidence: Basic Science Study; Computer Modeling

© 2023 The Author(s). This is an open access article under the CC BY license (<http://creativecommons.org/licenses/by/4.0/>).

Keywords: Transverse force couple; glenoid version; glenoid offset; scapulohumeral subluxation; rotator cuff muscles; muscle balance; nonpathological shoulders

Despite increasing studies focusing on scapulohumeral subluxation in the osteoarthritic shoulder,²⁷ the pathomechanics of static posterior subluxation of the humeral head (SPSH) and primary osteoarthritis with posterior decentering remain unclear.¹² Historically, SPSH has been described and classified in osteoarthritic conditions^{29,30,42} with frequent posterior erosion of the glenoid and SPSH. Recently, SPSH in young adults has been recognized as a condition resulting in glenohumeral osteoarthritis⁴¹ and referred to as preosteoarthritic SPSH or Walch B0.¹²

Bone anatomy has been studied in cases of SPSH, with a particular interest in the glenoid version,^{3,14,17,39} acromial anatomy,^{6,37} and scapular morphology.²² Initially described as a risk factor,⁴² the role of excessive glenoid retroversion, a static stabilizer of the glenohumeral joint,¹⁵ remains controversial in SPSH.^{12,17,22} Recently, Akgün et al.³ showed that young patients with preosteoarthritic SPSH present significant differences in bone anatomy, particularly increased anterior glenoid offset and excessive glenoid retroversion. Landau et al.²² discussed the genetic and biomechanical determinants of the scapula and glenoid vault morphology and showed large variations in glenoid version and glenoid translation. Hoenecke et al.¹⁷ found the same trend and, as in the previous study, questioned the role of glenoid orientation in SPSH, suggesting that soft tissue and muscle imbalance may be significant factors influencing SPSH. Other studies assumed that the variable relationship between the scapular body and glenoid vault may alter the relationship between the action lines of the rotator cuff muscles and result in SPSH.^{3,12,33,39}

There is growing interest in evaluating the rotator cuff muscle balance in glenohumeral osteoarthritis and shoulder instability,¹⁹ especially the transverse rotator cuff balance known as the transverse force couple (TFC), which includes the subscapularis anteriorly and the association of the infraspinatus and teres minor posteriorly. In nonpathological shoulders, the TFC is in balance, as shown by studies on muscle volume.^{8,13,32,40} Recent studies have reported varying results in the rotator cuff muscle volume^{4,10} and fatty infiltration,^{5,16} but they suggest a transverse

imbalance in posterior eccentric osteoarthritis. More recently, Bokor et al.⁷ questioned the variation in rotator cuff vectors in osteoarthritic shoulders with interesting results suggesting that glenoid retroversion is associated with variation in the orientation of shear and compression forces on the glenoid vault.

To the best of our knowledge, no studies have focused on the resultant force of the rotator cuff across the scapulohumeral joint in terms of scapulohumeral alignment and glenoid vault morphology in nonpathological shoulders. We hypothesized that the transverse resultant force of the 4 rotator cuff muscles, expressed as an angle in relation to the scapular blade axis, is associated with variation in the scapulohumeral subluxation index (SHSI) and glenoid vault morphology. The primary objective of this study was to evaluate the relationship between the transverse resultant force angle (TRFA) and SHSI. A further objective was to assess the relationship between the TRFA and selected bone parameters of the glenoid vault, as well as between each of the selected glenoid vault parameters.

Materials and methods

Study design and population

We retrospectively reviewed 443 consecutive patients who underwent a whole-body computed tomography (CT) scan between January 2020 and December 2020 in our level 1 trauma center. Inclusion criteria were female or male patients, over the age of 18, with CT images available for review. Exclusion criteria were any shoulder girdle fracture, pre-existing shoulder girdle pathology including glenohumeral osteoarthritis, previous shoulder surgery, presence of shoulder girdle hardware, patient position other than supine with arms at sides, incomplete CT coverage of the scapulohumeral region, and cases ineligible for analysis (lack of consent). Seventy-five single shoulders from 75 subjects were initially included. The arm rotation of each shoulder was analyzed in terms of the position of the bicipital groove at its middle level⁹ by a shoulder surgery fellow and an attending fellowship-trained shoulder surgeon. At this step, the exclusion criterion was

shoulders that were in internally or externally rotated based on the position of the bicipital groove at its middle level on CT. Fifty-five shoulders from 55 different patients were finally included in the analysis (Fig. 1). At the end of the case selection process, all CT images were deidentified to protect patient information according to the Institutional Review Board-approved study protocol.

Computed tomography protocol

Whole-body CT scans were performed using a 256-detector row CT system (Revolution CT; GE Healthcare, Waukesha, WI, USA). The relevant standardized data acquisition parameters were: tube potential, 120 kVp; tube current, ~150-400 mA; automatic exposure control, enabled; gantry revolution time, 0.5-0.6 seconds. The relevant parameters for image reconstruction were: field of view, $32 \times 32\text{-}40 \times 40 \text{ cm}^2$; section thickness, 1.25 mm.

Computed tomography landmarks

To define a scapular coordinate system, we used a fully automatic method³⁵ that placed 8 anatomical landmarks on 3-dimensional (3D) image reconstructions of the scapula. These landmarks were: angulus inferior, trigonum spinae, spinoglenoid notch, and 5 landmarks along the floor of the supraspinatus fossa. The scapular coordinate system comprised postero-anterior (X), medio-lateral (Z), and infero-superior (Y) axes, with the origin on the spino-glenoid notch landmark projected on the Z-axis (Fig. 2).

On the humeral head, we manually placed 11 landmarks (Fig. 3) using 3D Slicer (www.slicer.org): 5 landmarks (H1-H5) were used to determine the center and radius of the humeral head, and 6 landmarks were placed at the anatomical insertional footprints of the rotator cuff tendons.^{11,28} We first positioned 3 landmarks corresponding to i) the inferior end of the subscapularis insertion on the lesser tubercle, ii) the anterior end of the supraspinatus insertion next to the upper portion of the bicipital groove, and iii) the inferior end of the teres minor on the greater tubercle. Then, along the circular intersection between the plane fitted on these 3 landmarks and the humeral head surface, we defined the

adjacent tendon insertions by placing 3 further landmarks: iv) the superior end of the subscapularis insertion on the lesser tubercle next to the bicipital groove, v) the joint insertion shared by the supraspinatus and infraspinatus on the greater tubercle, and vi) the joint insertion shared by the infraspinatus and teres minor.

Transverse resultant force angle

The TRFA was defined as the angle between the (potential) force of the rotator cuff muscles and the scapular (Z) axis in the axial/transverse (ZX) plane (Fig. 4). This angle was positive when the rotator cuff muscle force was oriented posteriorly. A detailed description of this part of the method can be found in the [Supplementary Material](#). Briefly, each rotator cuff muscle was divided into a homogeneous density of virtual fibers (Fig. 5), and the fiber directions were evaluated between their position in the XY plane and their insertion on the humeral head or the tangential contact point. In the XY plane, the contours of each muscle were predicted by an automatic segmentation algorithm.³⁶ The virtual fiber vectors were then normalized, weighted by the muscle trophic ratio, and summed. The TRFA was calculated in 3D from the landmarks defined above, using a MATLAB code (www.mathworks.com).

Scapulohumeral subluxation index

The SHSI was measured in 3D as previously described by Terrier et al.^{38,39} as the relative distance between the humeral head center and glenoid center projected onto a plane perpendicular to the scapular axis. The SHSI was expressed in % as proposed by Walch et al.⁴²

Glenoid version angle

The glenoid version angle (GVA) was measured in 3D according to the method of Terrier et al.^{38,39} and calculated automatically.^{1,35} It was defined as the angle between the glenoid centerline and the scapular blade (Z) axis. The glenoid centerline was defined as the

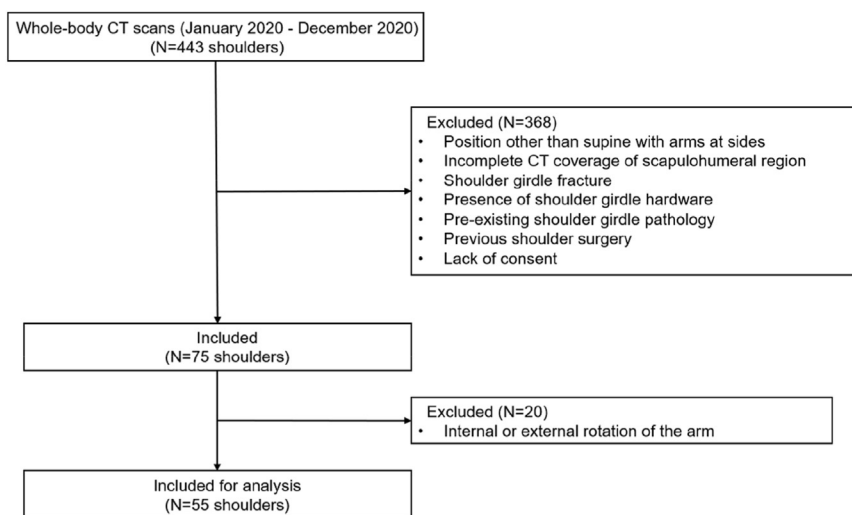


Figure 1 Patient selection flowchart. CT, computed tomography.

axis between the glenoid center point and the center of a sphere fitted on the glenoid fossa. The GVA was negative when facing backwards and positive when facing forwards (Fig. 4).

Glenoid anteroposterior offset angle

The glenoid anteroposterior offset angle (GOA) was inspired by Akgün et al.'s³ method for the neck angle. The GOA was defined as the angle between the scapular blade (Z) axis and the axis formed by the glenoid center C and the coordinate system origin. The GOA was positive when the glenoid presented anterior decentering compared to the scapular blade (Z) axis (Fig. 4).

Glenoid depth, width, and radius

The glenoid depth was defined as the distance from the glenoid center and the farthest glenoid surface points projected on the glenoid centerline. The glenoid width was defined as the distance between the 2 extreme values of the glenoid surface points projected on the axis of a principal component analysis (performed on the glenoid surface points) that was most aligned with the scapular posteroanterior (X) axis. The glenoid radius was the radius of the sphere fitted on the glenoid surface points.

Statistical analysis

We evaluated the associations between the TRFA and SHSI, GVA, GOA, glenoid depth, glenoid width, and glenoid radius using simple linear regression with the Pearson correlation coefficient (R). The Pearson correlation coefficient ranges from 1 (perfect positive linear correlation) to -1 (perfect negative linear correlation), with 0 indicating an absence of correlation. Correlation coefficients were interpreted as very strong (>0.9), strong (0.70-0.89), moderate (0.40-0.69), weak (0.10-0.39), or negligible (<0.10).³⁴ We tested the normal distribution of the variables using the Shapiro-Wilk test and sex-related differences using the Student's t -test for normally distributed variables and Wilcoxon rank-sum (Mann-Whitney) test for non-normally distributed variables. The sample size was based on the *a priori* power analysis estimating that 17 participants were needed when testing the null hypothesis regarding the TRFA based on an expected correlation coefficient of 0.7 between TRFA and SHSI ($\alpha = 0.05$, $\beta = 0.10$).³⁴ The statistical analysis was performed in R version 4.0 (www.R-project.org) with the mass library for stepwise multiple linear regression.

Results

Study population characteristics

Patient demographics

Fifty-five patients met the inclusion criteria, of which 55 shoulders were analyzed. There were no significant differences in age and body mass index between the 36 males and 19 females, but the height and weight distribution differed significantly between males and females ($P < .001$ and $P = .002$, respectively; Table I).

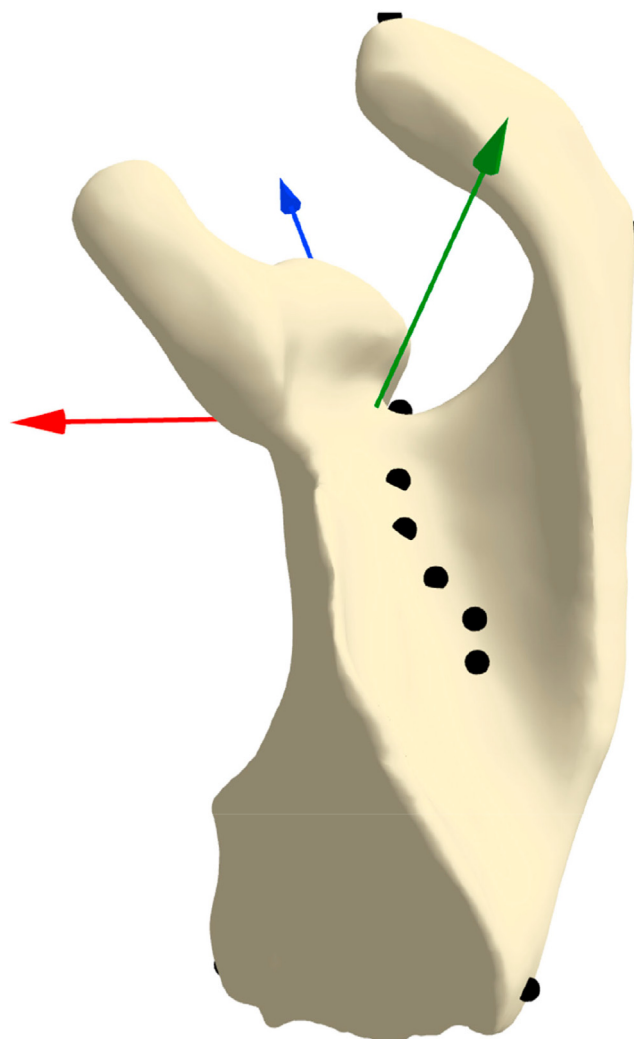


Figure 2 Placement of anatomical landmarks on the scapula to determine the scapular coordinate system: posteroanterior axis or X-axis (red arrow), inferosuperior axis or Y-axis (green arrow), mediolateral axis or Z-axis (blue arrow).

Distribution of biomechanical and anatomical parameters

The mean TRFA was $7.4 \pm 4.5^\circ$. The mean SHSI according to Walch was $54.3\% \pm 4.8\%$. The mean GVA and GOA were $-4.1 \pm 4.4^\circ$ and $5.1 \pm 10.8^\circ$, respectively. Regarding glenoid depth, glenoid width, and glenoid radius, the mean values were 3.3 ± 0.6 mm, 20 ± 2 mm, and 33.6 ± 4.6 mm, respectively (Table II).

Correlations

All correlations are reported in the correlation matrix (Fig. 6) and Table III.

Correlation between transverse resultant force angle and scapulohumeral subluxation index

We found a strong correlation between TRFA and SHSI ($R = -0.731$, $P < .001$).

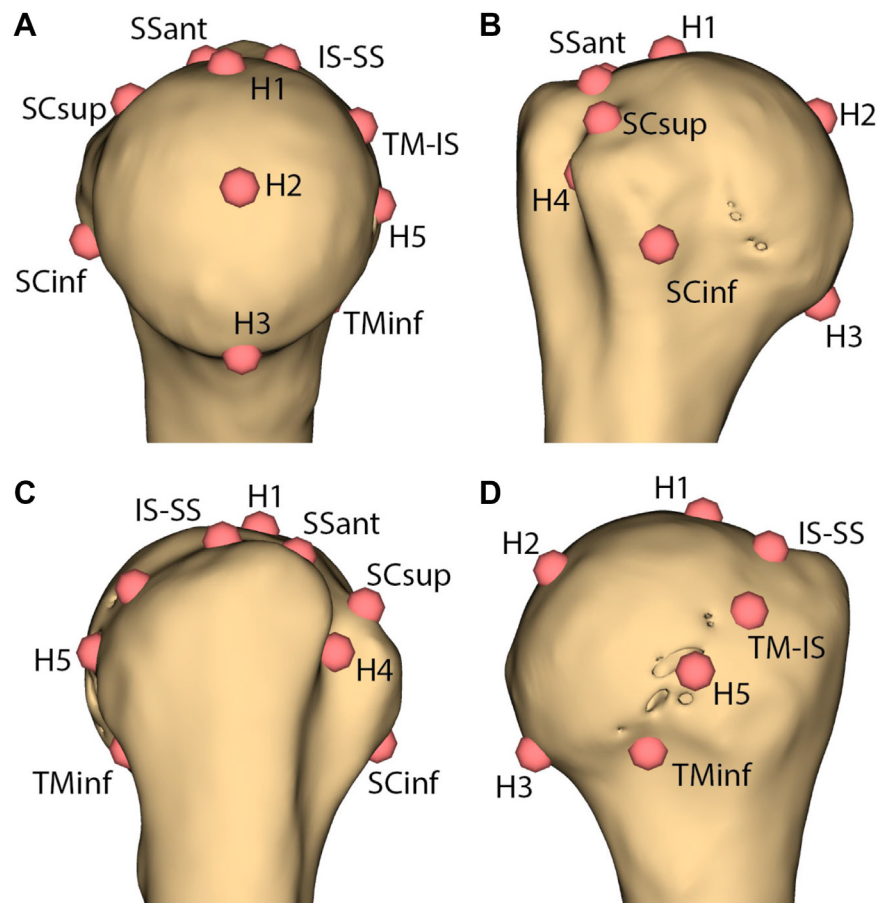


Figure 3 Placement of anatomical landmarks on the humeral head. Landmark positioning was performed on 3-dimensional (3D) image reconstructions in 3D Slicer. (A) Medial view, (B) anterior view, (C) lateral view, and (D) posterior view. (H1) Top of humeral articular best-fitting sphere in frontal plane, (H2) middle of humeral articular best-fitting sphere in frontal plane, (H3) bottom of humeral articular best-fitting sphere in frontal plane, (H4) intertubercular groove or sulcus, (H5) teres minor middle third. *SCinf*, subscapularis inferior; *SCsup*, subscapularis superior; *SSant*, supraspinatus anterior; *IS-SS*, infraspinatus-supraspinatus junction; *TM-IS*, teres minor-infraspinatus junction; *TMinf*, teres minor inferior.

Correlation between transverse resultant force angle and glenoid vault parameters

We found a strong correlation between TRFA and GVA ($R = 0.716$, $P < .001$) and a moderate correlation between TRFA and GOA ($R = 0.663$, $P < .001$) (Fig. 7). There was a negligible correlation between TRFA and glenoid depth ($R = 0.05$, $P = .369$), a weak negative correlation between TRFA and glenoid width ($R = -0.11$, $P = .339$), and a negligible correlation between TRFA and glenoid radius ($R = -0.01$, $P = .568$).

Correlation among glenoid vault parameters

We found a strong correlation between GVA and GOA ($R = 0.768$, $P < .001$). There were negligible or weak correlations between GVA, glenoid depth, glenoid width, and glenoid radius. The correlations between GOA, glenoid depth, glenoid width, and glenoid radius were also negligible or weak. We found a moderate correlation between glenoid depth and glenoid width ($R = 0.51$, $P = .001$), a weak correlation between glenoid depth and glenoid radius

($R = 0.24$, $P = .463$), and a strong correlation between glenoid width and glenoid radius ($R = 0.78$, $P < .001$).

Correlation between scapulohumeral subluxation index and glenoid vault parameters

We found a strong negative correlation between SHSI and GVA ($R = -0.813$, $P < .001$) and a moderate negative correlation between SHSI and GOA ($R = -0.552$, $P < .001$). There was a negligible correlation between SHSI and glenoid depth or glenoid radius ($R = -0.07$, $P = .034$ and $R = 0.03$, $P = .691$, respectively) and a weak negative correlation between SHSI and glenoid width ($R = -0.17$, $P = .193$).

Discussion

We hypothesized that the angle of the rotator cuff resultant force is associated with the scapulohumeral alignment and glenoid vault morphology in nonpathological shoulders. We

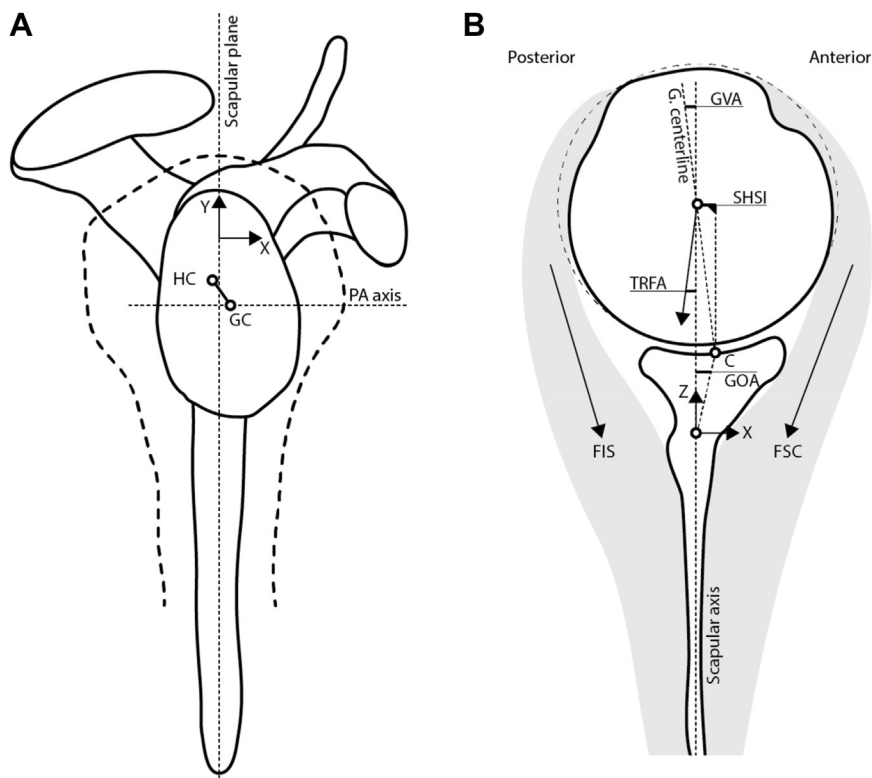


Figure 4 Schematic 2D representations of quantities measured in 3D. (A) Lateral view, (B) transverse view of the right shoulder. The scapular coordinate system is represented here by the X- and Z-axis. FIS and FSC represent the average force of the infraspinatus and subscapularis, respectively. *TRFA*, transverse resultant force angle; *SHSI*, scapulohumeral subluxation index; *GVA*, glenoid version angle; *GOA*, glenoid anteroposterior offset angle; *GC*, glenoid center; *HC*, humeral head center.

found a strong relationship between the *TRFA* and *SHSI*, meaning that increased posterior *SPSH* is associated with a decreased posterior angle of the rotator cuff resultant force in the transverse plane. Moreover, there was a strong relationship between the *TRFA*, *GVA*, and *GOA*, suggesting that an increased *TRFA* is associated with decreased glenoid retroversion and increased anterior offset of the glenoid vault. Furthermore, a strong relationship between glenoid version and anteroposterior glenoid offset implies that increased glenoid retroversion is associated with a decreased anterior glenoid offset in subjects with non-pathological shoulders.

In their landmark article focusing on the mechanisms of glenohumeral joint stability, Lipitt and Matsen²⁵ developed the concavity compression concept, which refers to the stability afforded to a convex object that is pressed into a concave surface, meaning that the dynamic compression of the humeral head into the glenoid fossa by the rotator cuff provides a stabilizing effect. In terms of shoulder biomechanics, static stability of the glenohumeral joint is provided by the glenoid bone anatomy and capsulolabral structures.¹⁵ Some studies focused on dynamic stability afforded by the long head of the biceps²⁰ or rotator cuff and other shoulder muscles,^{2,21,23,24,26} with special emphasis on the transverse plane. The “rotator cuff transverse force

couple” was described between the subscapularis anteriorly and the infraspinatus-teres minor combination posteriorly as a determining factor for normal shoulder function.¹⁸ Tingart et al.⁴⁰ studied the rotator cuff muscle volume on magnetic resonance imaging in 10 cadavers and showed that the volume between the subscapularis and the infraspinatus-teres minor couple was comparable. More recently, Piepers et al.³² evaluated the muscle volume of the TFC in 27 nonpathological shoulders on CT and found no significant differences between the volumes of the anterior and posterior TFC parts. Bouaicha et al.⁸ focused on the cross-sectional area of the rotator cuff muscles in 50 patients and reported a similar trend in the transverse volume balance. They concluded that their results support the biomechanical concept of a dynamically balanced shoulder in adults with intact rotator cuffs. Moreover, Espinosa-Urbe et al.¹³ showed that the volume ratio between the anterior and posterior parts of the TFC remains constant despite muscle atrophy. All these studies evaluated the TFC balance regarding the muscle volume assessed by different methods and imaging techniques. Some authors suggested that, in a shoulder with a balanced TFC, the resultant force of the anterior and posterior components is in line with the glenoid.^{25,31,32} Our results showed that, in nonpathological shoulders, there are variations in the angle of the resultant

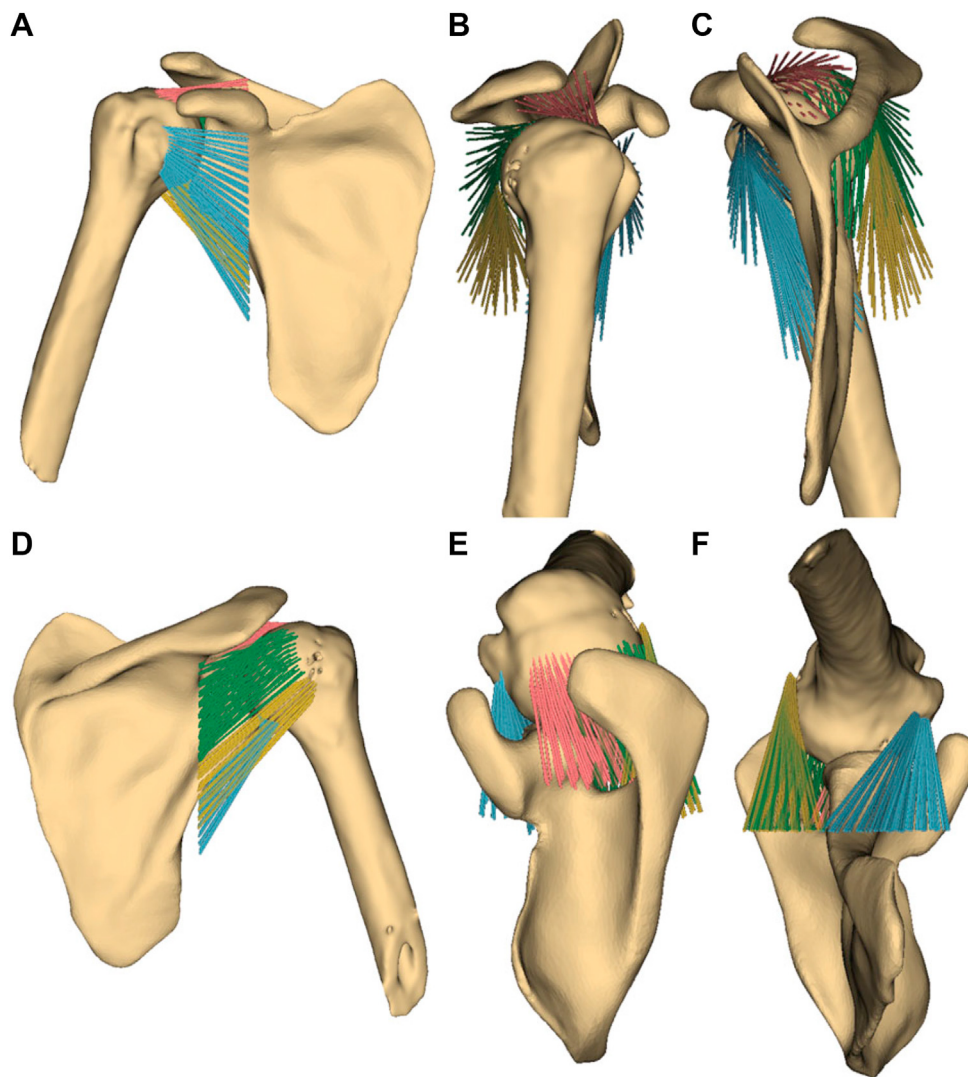


Figure 5 Representative example of the right shoulder of a 57-year-old male subject showing the muscle fibers of the rotator cuff: supraspinatus (red), subscapularis (blue), infraspinatus (green), and teres minor (yellow). The lateral fiber endings do not represent tendon insertions, but muscle action lines tangent to a sphere fitted on the humeral head. (A) Anterior view, (B) lateral view, (C) medial view, (D) posterior view, (E) superior view, and (F) inferior view.

Table I Patient characteristics

	Female, mean ± SD	Male, mean ± SD	<i>P</i> value
N	19	36	
Age (yr)	34.4 ± 13.5	40.1 ± 12.9	.130
Weight (kg)	69.4 ± 14.1	82.1 ± 12.6	.001
Height (cm)	165.5 ± 6.8	176.8 ± 7.3	<.001
BMI (kg/m ²)	25.1 ± 3.9	26.2 ± 3.1	.285

SD, standard deviation; *BMI*, body mass index.

transverse force of the rotator cuff across the scapulohumeral joint despite an assumed muscle volume balance. Furthermore, our findings seem to confirm Sabesan

et al.'s³³ hypothesis that a translated scapulohumeral alignment would likely alter the force vectors of the muscles crossing the glenohumeral joint.^{12,22,39}

Table II Distribution of scapulohumeral anatomical parameters

Variable	Mean \pm SD	95% CI	Median (IQR)	Min, max	95% percentile
TRFA (degree)	7.4 \pm 4.5	7.2, 7.6	7.3 (5.3)	-5.8, 19.1	-1.7, 16.5
SHSI (%)	54.3 \pm 4.8	54.1, 54.5	54.0 (5.1)	45.1, 67.6	44.6, 64.0
GVA (degree)	-4.1 \pm 4.4	-4.3, -4.0	-3.6 (5.8)	-15.5, 3.2	-12.9, 4.6
GOA (degree)	5.1 \pm 10.8	4.7, 5.5	3.9 (15.4)	-16, 29.4	-16.5, 26.6
Glenoid depth (mm)	3.3 \pm 0.6	3.3, 3.4	3.3 (0.7)	2.2, 4.6	2.2, 4.4
Glenoid width (mm)	20.0 \pm 2.0	19.9, 20.1	20.2 (3.2)	16.4, 23.3	16.0, 24.0
Glenoid radius (mm)	33.6 \pm 4.6	33.4, 33.7	34.2 (6.8)	25.4, 44.4	24.3, 42.8

TRFA, Transverse resultant force angle; SHSI, scapulohumeral subluxation index; GVA, glenoid version angle; GOA, glenoid anteroposterior offset angle; SD, standard deviation; CI, confidence interval; IQR, interquartile range.

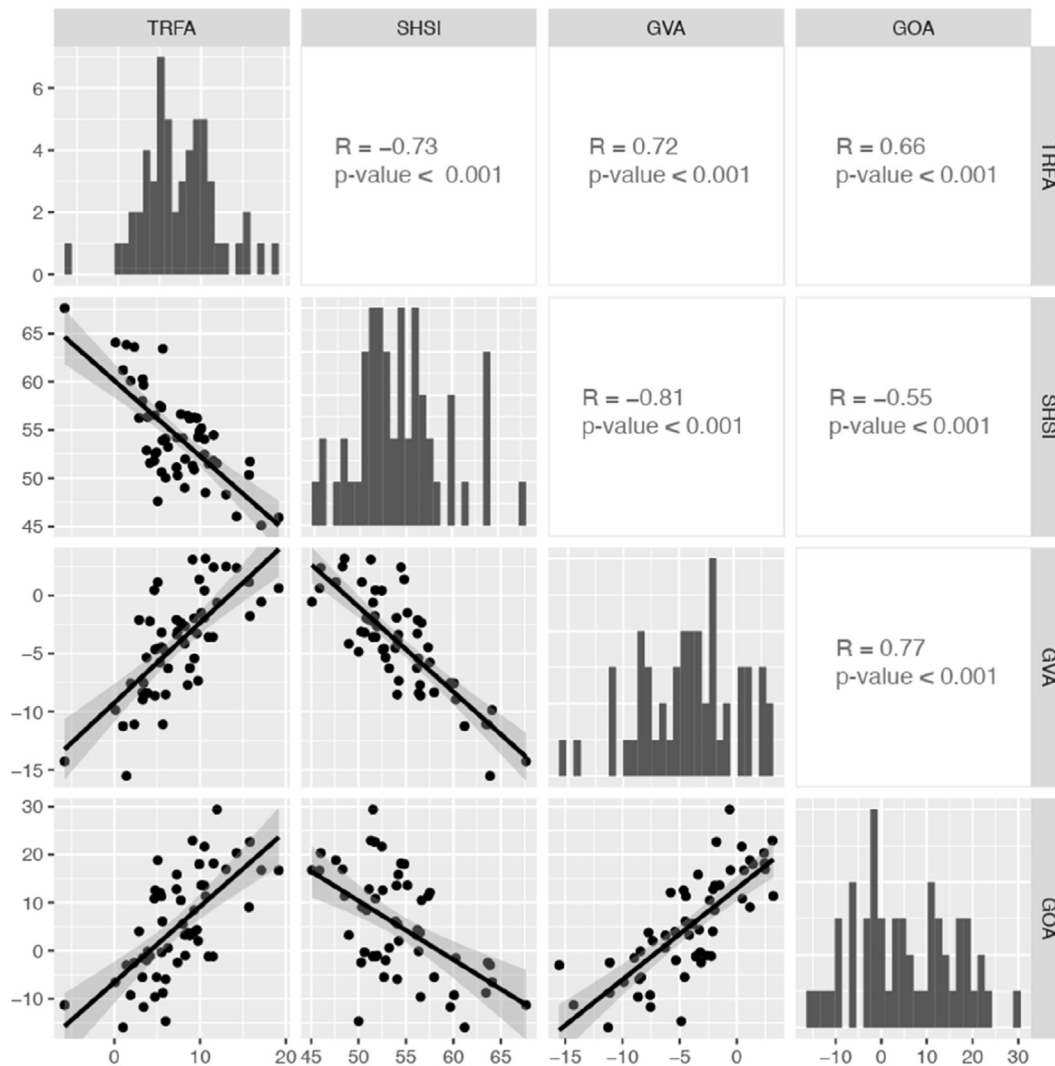


Figure 6 Correlation matrix between TRFA, SHSI, GVA, and GOA. TRFA, transverse resultant force angle; SHSI, scapulohumeral subluxation index; GVA, glenoid version angle; GOA, glenoid anteroposterior offset angle; R, Pearson correlation coefficient.

Akgün et al.³ recently studied the glenoid vault and scapulohumeral alignment in young patients with SPSH compared to a control group and showed that patients with SPSH had significantly increased anterior glenoid offset,

excessive glenoid retroversion, and increased posterior humeral head offset. They assumed that the glenoid vault morphology, especially the anterior glenoid offset, could alter the action line of the rotator cuff muscles. We found a

Table III Correlations between quantities.

	TRFA	SHSI	GVA	GOA	GR	GW	GD	Age	Height	Weight
TRFA	1	-0.73	0.72	0.66	0.08	-0.13	-0.12	-0.02	-0.21	-0.19
SHSI	<0.001	1	-0.81	-0.55	-0.05	0.18	0.29	0.05	0.27	0.26
GVA	<0.001	<0.001	1	0.77	-0.04	-0.17	-0.16	-0.01	-0.22	-0.15
GOA	<0.001	<0.001	<0.001	1	-0.09	-0.14	-0.02	-0.22	-0.2	-0.11
GR	0.568	0.691	0.777	0.532	1	0.69	-0.1	0.22	0.45	0.35
GW	0.339	0.193	0.216	0.301	<0.001	1	0.43	0.39	0.67	0.56
GD	0.369	0.034	0.242	0.880	0.463	0.001	1	0.23	0.35	0.23
Age	0.871	0.737	0.917	0.114	0.108	0.003	0.091	1	0.23	0.38
Height	0.128	0.050	0.113	0.147	0.001	<0.001	0.009	0.086	1	0.75
Weight	0.157	0.052	0.289	0.404	0.009	<0.001	0.095	0.004	<0.001	1

TRFA, transverse resultant force angle; SHSI, scapulohumeral subluxation index; GVA, glenoid version angle; GOA, glenoid anteroposterior offset angle; GD, glenoid depth; GW, glenoid width; GR, glenoid radius.

Values above the diagonal are pearson correlation coefficients (R), values below the diagonal are *P* values.

strong correlation between the TRFA and glenoid offset, meaning that an increased anterior glenoid offset was associated with an increased angle of the rotator cuff resultant force to the scapular axis. In their review, Doms et al.¹² focused on Walch B0 glenoids and highlighted the possible multifactorial causes of SPSH related to soft tissue and bone factors, as conflicting results have been reported regarding the relationship between glenoid retroversion and scapulohumeral subluxation.^{3,14,17,22,39} We reported a strong correlation between glenoid version and the resultant force angle, meaning that increased glenoid retroversion was associated with a decreased posterior TRFA. Nyffeler et al.³¹ were interested in the variation in joint reaction forces to glenoid component version. They found that for every 4° change in retroversion, there was a 2° change in the posterior orientation of the force vector. These divergent results compared to our study may be due to differences in measurement methods and the variation in glenoid version with other anatomical parameters, especially the anterior glenoid offset. The lack of correlation between the angle of the resultant force and glenoid depth, glenoid width, and glenoid radius may be due to the static evaluation of the scapulohumeral region.

Landau et al.²² highlighted the wide variability in scapular bone anatomy through the modular scapula concept, which corresponded to the variations in normal scapular morphology in terms of body shape, glenoid translation, and glenoid version, depending on gene regulation, especially that of *Emx2* and *HOXC6*. In the control group, Akgün et al.³ reported a mean glenoid neck angle and glenoid offset of 173° and 4.6 mm, respectively. The present study highlighted a strong correlation concerning their variation. Interestingly, and as described previously, Akgün et al.³ indicated that the SPSH group demonstrated significantly increased glenoid retroversion and anterior glenoid offset compared to healthy shoulders. The association of these 2 variations with regard to increased glenoid retroversion and anterior offset, which seems to not

correlate in our nonpathological shoulders, could be an essential constitutional difference. Moreover, our results suggest that an increased anterior glenoid offset correlated with a decreased SHSI in our healthy shoulders compared to the SPSH group reported by Akgün et al.,³ who found that posterior subluxation of the humerus was associated with an increased anteriorly displaced glenoid. As previously described by Terrier et al.,³⁹ we also showed a strong correlation between increased glenoid retroversion and an increased SHSI, which remains debated in the literature.^{12,17,22}

Our results support the hypothesis of other authors that the scapulohumeral alignment could alter the resultant force across the glenohumeral joint. In osteoarthritic conditions, Bokor et al.⁷ showed the same trend with stimulating results regarding the variation in rotator cuff vectors between Walch types A and B. Their results highlighted that increased glenoid retroversion is associated with increased posterior shear force and decreased compression force on the glenoid fossa, with a special interest in the infraspinatus-teres minor couple and supraspinatus, for which increased retroversion could change an anterior thrust to a posterior drag. The role of the muscle forces, especially those concerning the rotator cuff, across the scapulohumeral joint is not fully understood despite several studies being interested in it. Further studies focusing on dynamic evaluation of the force across the shoulder joint are required to highlight the link between the force variations in nonpathological shoulders and pathological conditions.

Our study has some limitations. First, we conducted an evaluation based on motionless shoulders imaged by CT. Despite our meticulous method to estimate each rotator cuff tendon's anatomical insertion and related muscle force vector, minor variations may affect correlations. Furthermore, rotator cuff muscle volumes were assessed by successive cross-sectional areas in a single plane, which could affect the volume evaluation. We did not consider the other

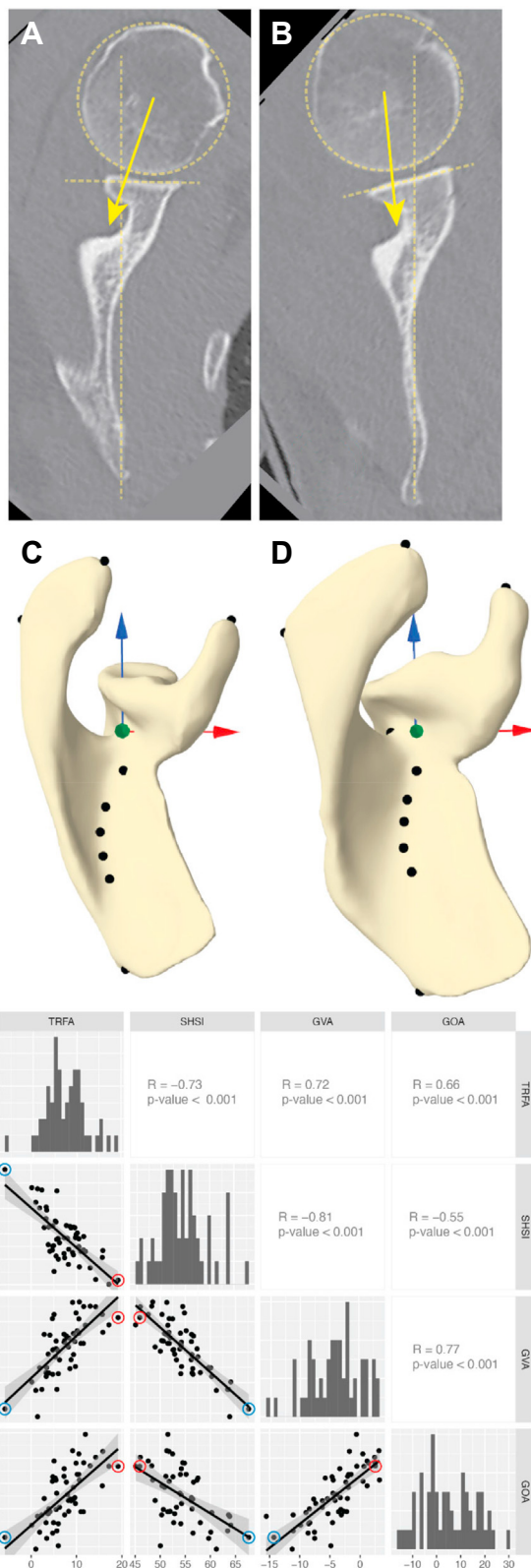


Figure 7 Illustration of 2 contrasting cases. Computed tomography scans of a 41-year-old female (Case 1; **A** and **C**) and a 45-year-old male (Case 2; **B** and **D**) with representation of the TRFA (yellow arrow) and corresponding superior views of the scapula. (Correlation matrix) Parameter values for case 1 (○) and case 2

muscles that intersect with the shoulder joint, such as the deltoid, pectoralis major, latissimus dorsi, or teres major.² These muscles may affect the resultant force of the scapulohumeral joint. Finally, our retrospective study included patients with whole-body CT scans performed in the emergency department for various traumas. Despite comprehensive inclusion and exclusion criteria, no additional imaging (magnetic resonance imaging or ultrasound) was available to definitely exclude any underlying pathological conditions of the shoulder joint.

Conclusion

Our findings suggest the presence of variations in the rotator cuff resultant force in the transverse plane, despite a previously demonstrated transverse muscle volume balance. Variations in the glenoid vault parameters and scapulohumeral subluxation influence the direction of the rotator cuff resultant force. Moreover, we found a strong correlation between the glenoid version and the anterior glenoid offset, implying that increased glenoid retroversion is associated with a decreased anterior glenoid offset in nonpathological shoulders. The rotator cuff reaction force may help characterize the variability and intercorrelation of clinically relevant scapular morphology parameters and scapulohumeral alignment. These results could be useful in understanding subsequent pathological changes.

Disclaimers:

Funding: This study was supported by the Swiss National Science Foundation (SNF 189972) and the “Lausanne Orthopedic Research Foundation” (LORF). **Conflicts of interest:** The authors, their immediate families, and any research foundation with which they are affiliated have not received any financial payments or other benefits from any commercial entity related to the subject of this article.

Supplementary Data

Supplementary data to this article can be found online at <https://doi.org/10.1016/j.jse.2023.09.031>.

(○). (vertical yellow dotted line) Scapular axis. (horizontal yellow dotted line) Glenoid axis. TRFA, transverse resultant force angle; SHSI, scapulohumeral subluxation index; GVA, glenoid version angle; GOA, glenoid anteroposterior offset angle; R, Pearson correlation coefficient.

References

- Abler D, Berger S, Terrier A, Becce F, Farron A, Büchler P. A statistical shape model to predict the premorbid glenoid cavity. *J Shoulder Elbow Surg* 2018;27:1800-8. <https://doi.org/10.1016/j.jse.2018.04.023>
- Ackland DC, Pandy MG. Lines of action and stabilizing potential of the shoulder musculature. *J Anat* 2009;215:184-97. <https://doi.org/10.1111/j.1469-7580.2009.01090.x>
- Akgün D, Siegert P, Danzinger V, Plachel F, Minkus M, Thiele K, et al. Glenoid vault and humeral head alignment in relation to the scapular blade axis in young patients with pre-osteoarthritic static posterior subluxation of the humeral head. *J Shoulder Elbow Surg* 2021;30:756-62. <https://doi.org/10.1016/j.jse.2020.08.004>
- Aleem AW, Chalmers PN, Bechtold D, Khan AZ, Tashjian RZ, Keener JD. Association between rotator cuff muscle size and glenoid deformity in primary glenohumeral osteoarthritis. *J Bone Joint Surg Am* 2019;101:1912-20. <https://doi.org/10.2106/JBJS.19.00086>
- Arenas-Miquelez A, Liu VK, Cavanagh J, Graham PL, Ferreira LM, Bokor DJ, et al. Does the Walch type B shoulder have a transverse force couple imbalance? A volumetric analysis of segmented rotator cuff muscles in osteoarthritic shoulders. *J Shoulder Elbow Surg* 2021;30:2344-54. <https://doi.org/10.1016/j.jse.2021.02.005>
- Beeler S, Hasler A, Götschi T, Meyer DC, Gerber C. Different acromial roof morphology in concentric and eccentric osteoarthritis of the shoulder: a multiplane reconstruction analysis of 105 shoulder computed tomography scans. *J Shoulder Elbow Surg* 2018;27:e357-66. <https://doi.org/10.1016/j.jse.2018.05.019>
- Bokor DJ, Arenas-Miquelez A, Axford D, Graham PL, Ferreira LM, Athwal GS, et al. Does the osteoarthritic shoulder have altered rotator cuff vectors with increasing glenoid deformity? - an in-silico analysis. *J Shoulder Elbow Surg* 2022;31:e575-85. <https://doi.org/10.1016/j.jse.2022.06.008>
- Bouaicha S, Slankamenac K, Moor BK, Tok S, Andreisek G, Finkenstaedt T. Cross-sectional area of the rotator cuff muscles in MRI - is there evidence for a biomechanical balanced shoulder? *PLoS One* 2016;11:e0157946. <https://doi.org/10.1371/journal.pone.0157946>
- Buck FM, Dietrich TJ, Resnick D, Jost B, Pfirrmann CWA. Long biceps tendon: normal position, shape, and orientation in its groove in neutral position and external and internal rotation. *Radiology* 2011;261:872-81. <https://doi.org/10.1148/radiol.11110914>
- Chalmers PN, Beck L, Miller M, Stertz I, Henninger HB, Tashjian RZ. Glenoid retroversion associates with asymmetric rotator cuff muscle atrophy in those with Walch B-type glenohumeral osteoarthritis. *J Am Acad Orthop Surg* 2020;28:547-55. <https://doi.org/10.5435/JAAOS-D-18-00830>
- Curtis AS, Burbank KM, Tierney JJ, Scheller AD, Curran AR. The insertional footprint of the rotator cuff: an anatomic study. *Arthroscopy* 2006;22:609.e1. <https://doi.org/10.1016/j.arthro.2006.04.001>
- Domos P, Checchia CS, Walch G. Walch B0 glenoid: pre-osteoarthritic posterior subluxation of the humeral head. *J Shoulder Elbow Surg* 2018;27:181-8. <https://doi.org/10.1016/j.jse.2017.08.014>
- Espinosa-Urbe AG, Negreros-Osuna AA, Gutiérrez-de la O J, Vílchez-Cavazos F, Pinales-Razo R, Quiroga-Garza A, et al. An age- and gender-related three-dimensional analysis of rotator cuff transverse force couple volume ratio in 304 shoulders. *Surg Radiol Anat* 2017;39:127-34. <https://doi.org/10.1007/s00276-016-1714-x>
- Gerber C, Costouros JG, Sukthankar A, Fucentese SF. Static posterior humeral head subluxation and total shoulder arthroplasty. *J Shoulder Elbow Surg* 2009;18:505-10. <https://doi.org/10.1016/j.jse.2009.03.003>
- Goetti P, Denard PJ, Collin P, Ibrahim M, Hoffmeyer P, Lädermann A. Shoulder biomechanics in normal and selected pathological conditions. *EFORT Open Rev* 2020;5:508-18. <https://doi.org/10.1302/2058-5241.5.200006>
- Hartwell MJ, Harold RE, Sweeney PT, Seitz AL, Marra G, Saltzman MD. Imbalance in axial-plane rotator cuff fatty infiltration in posteriorly worn glenoids in primary glenohumeral osteoarthritis: an MRI-based study. *Clin Orthop* 2021;479:2471-9. <https://doi.org/10.1097/CORR.0000000000001798>
- Hoenecke HR, Tibor LM, D'Lima DD. Glenoid morphology rather than version predicts humeral subluxation: a different perspective on the glenoid in total shoulder arthroplasty. *J Shoulder Elbow Surg* 2012;21:1136-41. <https://doi.org/10.1016/j.jse.2011.08.044>
- Hsu JE, Reuther KE, Sarver JJ, Lee CS, Thomas SJ, Glaser DL, et al. Restoration of anterior-posterior rotator cuff force balance improves shoulder function in a rat model of chronic massive tears. *J Orthop Res* 2011;29:1028-33. <https://doi.org/10.1002/jor.21361>
- Ishikawa H, Smith KM, Wheelwright JC, Christensen GV, Henninger HB, Tashjian RZ, et al. Rotator cuff muscle imbalance associates with shoulder instability direction. *J Shoulder Elbow Surg* 2022;32:33-40. <https://doi.org/10.1016/j.jse.2022.06.022>
- Itoi E, Newman SR, Kuechle DK, Morrey BF, An KN. Dynamic anterior stabilisers of the shoulder with the arm in abduction. *J Bone Joint Surg Br* 1994;76:834-6.
- Labriola JE, Lee TQ, Debski RE, McMahon PJ. Stability and instability of the glenohumeral joint: the role of shoulder muscles. *J Shoulder Elbow Surg* 2005;14(1 Suppl S):32S-8S. <https://doi.org/10.1016/j.jse.2004.09.014>
- Landau JP, Hoenecke HR. Genetic and biomechanical determinants of glenoid version: implications for glenoid implant placement in shoulder arthroplasty. *J Shoulder Elbow Surg* 2009;18:661-7. <https://doi.org/10.1016/j.jse.2008.11.012>
- Lee SB, An KN. Dynamic glenohumeral stability provided by three heads of the deltoid muscle. *Clin Orthop* 2002;400:40-7. <https://doi.org/10.1097/00003086-200207000-00006>
- Lee SB, Kim KJ, O'Driscoll SW, Morrey BF, An KN. Dynamic glenohumeral stability provided by the rotator cuff muscles in the mid-range and end-range of motion. A study in cadavera. *J Bone Joint Surg Am* 2000;82:849-57.
- Lippitt S, Matsen F. Mechanisms of glenohumeral joint stability. *Clin Orthop* 1993;291:20-8.
- Lippitt SB, Vanderhooft JE, Harris SL, Sidles JA, Harryman DT, Matsen FA. Glenohumeral stability from concavity-compression: a quantitative analysis. *J Shoulder Elbow Surg* 1993;2:27-35.
- Matsen FA, Hsu JE. Subluxation in the arthritic shoulder. *JBJS Rev* 2021;9:e21.00102. <https://doi.org/10.2106/JBJS.RVW.21.00102>
- Mochizuki T, Sugaya H, Uomizu M, Maeda K, Matsuki K, Sekiya I, et al. Humeral insertion of the supraspinatus and infraspinatus. New anatomical findings regarding the footprint of the rotator cuff. *J Bone Joint Surg Am* 2008;90:962-9. <https://doi.org/10.2106/JBJS.G.00427>
- Neer CS. Replacement arthroplasty for glenohumeral osteoarthritis. *J Bone Joint Surg Am* 1974;56:1-13.
- Neer CS, Morrison DS. Glenoid bone-grafting in total shoulder arthroplasty. *J Bone Joint Surg Am* 1988;70:1154-62.
- Nyffeler RW, Sheikh R, Atkinson TS, Jacob HAC, Favre P, Gerber C. Effects of glenoid component version on humeral head displacement and joint reaction forces: an experimental study. *J Shoulder Elbow Surg* 2006;15:625-9. <https://doi.org/10.1016/j.jse.2005.09.016>
- Piepers I, Boudt P, Van Tongel A, De Wilde L. Evaluation of the muscle volumes of the transverse rotator cuff force couple in non-pathologic shoulders. *J Shoulder Elbow Surg* 2014;23:e158-62. <https://doi.org/10.1016/j.jse.2013.09.027>
- Sabesan VJ, Callanan M, Youderian A, Iannotti JP. 3D CT assessment of the relationship between humeral head alignment and glenoid retroversion in glenohumeral osteoarthritis. *J Bone Joint Surg Am* 2014;96:e64. <https://doi.org/10.2106/JBJS.L.00856>
- Schober P, Boer C, Schwarte LA. Correlation coefficients: appropriate use and interpretation. *Anesth Analg* 2018;126:1763-8. <https://doi.org/10.1213/ANE.0000000000002864>
- Taghizadeh E, Terrier A, Becce F, Farron A, Büchler P. Automated CT bone segmentation using statistical shape modelling and local template matching. *Comput Methods Biomech Biomed Engin* 2019;22:1303-10. <https://doi.org/10.1080/10255842.2019.1661391>

36. Taghizadeh E, Truffer O, Becce F, Eminian S, Gidoïn S, Terrier A, et al. Deep learning for the rapid automatic quantification and characterization of rotator cuff muscle degeneration from shoulder CT datasets. *Eur Radiol* 2021;31:181-90. <https://doi.org/10.1007/s00330-020-07070-7>
37. Terrier A, Becce F, Vauclair F, Farron A, Goetti P. Association of the posterior acromion extension with glenoid retroversion: a CT study in normal and osteoarthritic shoulders. *J Clin Med* 2022;11:351. <https://doi.org/10.3390/jcm11020351>
38. Terrier A, Goetti P, Becce F, Farron A. Reduction of scapulohumeral subluxation with posterior augmented glenoid implants in anatomic total shoulder arthroplasty: short-term 3D comparison between pre- and post-operative CT. *Orthop Traumatol Surg Res* 2020;106:681-6. <https://doi.org/10.1016/j.otsr.2020.03.007>
39. Terrier A, Ston J, Farron A. Importance of a three-dimensional measure of humeral head subluxation in osteoarthritic shoulders. *J Shoulder Elbow Surg* 2015;24:295-301. <https://doi.org/10.1016/j.jse.2014.05.027>
40. Tingart MJ, Apreleva M, Lehtinen JT, Capell B, Palmer WE, Warner JJP. Magnetic resonance imaging in quantitative analysis of rotator cuff muscle volume. *Clin Orthop* 2003;415:104-10. <https://doi.org/10.1097/01.blo.0000092969.12414.e1>
41. Walch G, Ascari C, Boulahia A, Nové-Josserand L, Edwards TB. Static posterior subluxation of the humeral head: an unrecognized entity responsible for glenohumeral osteoarthritis in the young adult. *J Shoulder Elbow Surg* 2002;11:309-14. <https://doi.org/10.1067/mse.2002.124547>
42. Walch G, Badet R, Boulahia A, Khoury A. Morphologic study of the glenoid in primary glenohumeral osteoarthritis. *J Arthroplasty* 1999; 14:756-60.